Proc. Roy. Soc. Lond. A. **316**, 153–167 (1970)
Printed in Great Britain

On kinematic dynamos

BY F. E. M. LILLEY
Department of Geophysics and Geochemistry, Australian National University, Canberra, A.C.T., Australia

(*Communicated by Sir Edward Bullard, F.R.S.—Received* 28 *August* 1969)

The method developed by Bullard & Gellman, to test flows of electrically conducting fluid in a sphere for dynamo action, is applied further to the two-component $T_1S_2^{2c}$ flow pattern they proposed. In agreement with Gibson & Roberts, it is found that the results of the test are negative, which substantiates the indication from Braginskii's work that the $T_1S_2^{2c}$ flow pattern has too great a symmetry for it to act as a dynamo. However, the addition of a third component, S_2^{2s}, to the flow pattern reduces the symmetry and produces results which indicate strongly that the three-component $T_1S_2^{2c}S_2^{2s}$ flow does act as a dynamo. Harmonics of magnetic field up to degree six have been taken into account, and this level of truncation appears to be justified. The streamlines of the $T_1S_2^{2c}S_2^{2s}$ flow form a distinctive whirling pattern in three dimensions, and this may be a physical characteristic necessary for dynamo action.

The main magnetic fields of the $T_1S_2^{2c}S_2^{2s}$ dynamo are all toroidal, and the possibility is established that the geomagnetic dynamo is similar, with the dominant components of field being completely contained within the core. Variation of the subsidiary poloidal components of the field may then produce secular variation and even dipole reversals, without major change in the series of interactions between the toroidal components that form the basic dynamo.

1. INTRODUCTION

A homogeneous dynamo is one in which a body of fluid conductor flows in such a way as to maintain a magnetic field by electromagnetic induction. In the kinematic problem, the flow pattern of the fluid is prescribed, without reference to the hydrodynamic equations.

The problem of the possible existence of such homogeneous dynamos is fascinating from the physical point of view, as well as being crucial to geomagnetism as a mechanism to maintain the magnetic field of the Earth. That they can indeed exist was first established on theoretical grounds by Backus (1958) and Herzenberg (1958). Since then, an experimental dynamo of the Herzenberg type has been successfully constructed by Lowes & Wilkinson (1963, 1968). While these cases prove that certain rather special patterns of motion will maintain dynamo action, whole classes of other flow patterns are excluded by the general theorems of Cowling (1933), Elsasser (1946), Bullard & Gellman (1954) and Lortz (1968). What is not clear at present is the full set of criteria that a flow must satisfy for it to be a possible dynamo: existence theorems have generally been restricted to special cases.

This paper is particularly concerned with the early analysis of the problem by Bullard & Gellman (1954), which provided a method for testing any flow pattern numerically, to see if it could exhibit dynamo action. At that time the storage capacity of computing machines severely limited the application of the method, even in the case of the simple flow pattern of two components that Bullard & Gellman chose to test.

The speed and storage capacities of available computers have since increased more than a thousandfold, and Gibson & Roberts (1969) have extended the work on the Bullard & Gellman model, with results inconclusive as to whether it really does act as a steady dynamo. However, the main contribution of the Bullard & Gellman paper lay in providing a method of attack which is, of course, quite general in application. This paper reports the results of testing, with the Bullard & Gellman procedure, a new flow pattern, obtained from the previous one by adding a third component of flow. Computing machine storage is still a limitation; the test has however been taken sufficiently far for the results to show excellent indications of convergence, which is the criterion for steady dynamo action.

2. The Bullard–Gellman analysis of the problem

Only a brief outline of the method is given here, as more details of it may be found in Gibson & Roberts (1969) as well as in the original paper. Expressing the magnetic field by $\boldsymbol{H}$, the electrical conductivity by σ, the permeability by μ, the velocity by $\boldsymbol{u}$, and time by t, the electromagnetic induction equation, in m.k.s. units, is

$$\nabla^2 \boldsymbol{H} = \sigma\mu \left[\frac{\partial \boldsymbol{H}}{\partial t} - \operatorname{curl}(\boldsymbol{u}\times\boldsymbol{H})\right]. \tag{1}$$

This is now put into a dimensionless form. Distance is scaled in terms of the radius, a, of the spherical body of conducting fluid in which dynamo action is being sought. Time is scaled in units of $\sigma\mu a^2$, and so velocity in units of $(\sigma\mu a)^{-1}$. For the case of steady dynamo action, dealt with here, the derivative of $\boldsymbol{H}$ with respect to time is zero, and equation (1) may be written

$$\nabla^2 \boldsymbol{H} + V \operatorname{curl}(\boldsymbol{v}\times\boldsymbol{H}) = 0. \tag{2}$$

The dimensionless velocity has been expressed as the product of a scalar V, giving the relative 'speed' of the flow, and a velocity field $\boldsymbol{v}$, defining the form of the flow pattern. In terms of V and $\boldsymbol{v}$, the velocity of the motion in m/s is

$$\boldsymbol{u}(r,\theta,\phi) = \frac{V\boldsymbol{v}(r,\theta,\phi)}{\sigma\mu a}.$$

The fluid is taken to be incompressible, so $\operatorname{div}\boldsymbol{v} = 0$. In addition, from electromagnetic theory, $\operatorname{div}\boldsymbol{H} = 0$. It is therefore possible to expand $\boldsymbol{v}$ and $\boldsymbol{H}$ in terms of poloidal and toroidal spherical harmonics, each of which automatically satisfies the condition of zero divergence. These spherical harmonics are vector fields, a toroidal one being denoted

$$\boldsymbol{T} = T_\theta\hat{\theta} + T_\phi\hat{\phi}$$

and a poloidal one

$$\boldsymbol{S} = S_r\hat{r} + S_\theta\hat{\theta} + S_\phi\hat{\phi}.$$

They are derived from simple scalar functions of radius, denoted by $T(r)$ if generating a toroidal field, and $S(r)$ if generating a poloidal field, in the following manner:

$$T_r = 0, \quad T_\theta = \frac{T(r)}{r\sin\theta}\frac{\partial Y}{\partial\phi}, \quad T_\phi = -\frac{T(r)}{r}\frac{\partial Y}{\partial\theta},$$

$$S_r = \frac{n(n+1)}{r^2}S(r)\,Y, \quad S_\theta = \frac{1}{r}\frac{\partial S(r)}{\partial r}\frac{\partial Y}{\partial\theta}, \quad S_\phi = \frac{1}{r\sin\theta}\frac{\partial S(r)}{\partial r}\frac{\partial Y}{\partial\phi}.$$

Here Y is the surface harmonic $P_n^m(\cos\theta)^{\sin}_{\cos}\,m\phi$, the unnormalized Ferrer's form being used. Thus, for example, the $\boldsymbol{T}_n^{mc}$ component of a vector field is derived from the Y_n^{mc} harmonic and the appropriate radial function, which, if described in full, would be $T_n^{mc}(r)$.

For simplicity, comprehensive suffix labels are also used, and thus the velocity is expanded as

$$\boldsymbol{v} = \sum_\alpha (\boldsymbol{S}_\alpha + \boldsymbol{T}_\alpha)$$

and the magnetic field as

$$\boldsymbol{H} = \sum_\beta (\boldsymbol{S}_\beta + \boldsymbol{T}_\beta).$$

Now in the terms of the kinematic problem $\boldsymbol{v}$ is specified, and the sum over α is therefore finite and known. The task is to find the corresponding value for V and the solution for $\boldsymbol{H}$. The series for $\boldsymbol{H}$ is, in general, infinite. In the numerical treatment of the problem it has to be truncated, and the crucial point is whether this can be done with justification, meaning that the terms ignored are unimportant. The approach is therefore to solve the problem a number of times, with the series for $\boldsymbol{H}$ truncated at successively higher levels; if the solution stabilizes, this is taken as strong evidence that the truncation is justified, and that the series for $\boldsymbol{H}$ has converged.

Although the notation is cumbersome, and infinite series become involved, the expansions given above for $\boldsymbol{v}$ and $\boldsymbol{H}$ result in a considerable simplification of the problem. Though of simple appearance, the vector induction equation (2) is equivalent to a formidable set of three scalar partial differential equations in three independent variables. When spherical harmonics are used, however, certain properties they have enable a treatment of vector derivatives and cross products, such that the induction equation reduces instead to a set of relatively simple ordinary differential equations. There is an equation for the radial function of every magnetic component considered, and except in trivial cases, which are known not to act as dynamos, the set of equations is infinite because the series for $\boldsymbol{H}$ is infinite. Upon truncation of the series for $\boldsymbol{H}$, the set of equations is also truncated, and solutions of the problem may be obtained numerically.

3. The computing routine

The burden of the present work has been to assemble a computing routine for automatically carrying out the Bullard & Gellman analysis on any postulated flow. The procedure is as follows. The flow components, of which there can in principle be any number, are each checked to find what interactions they cause between different magnetic field components. The level of truncation of the series for $\boldsymbol{H}$ is chosen, and all higher harmonics are ignored. Every interaction is evaluated, and noted as a contribution to the magnetic component it produces. This forms the set of ordinary differential equations corresponding to the induction equation. To solve these numerically, the differential equations are first approximated by difference equations at equally spaced points over the range of radius. Equation (2) is then in the form of a matrix eigenvalue problem, in which the eigenvalues are for V, and the eigenvectors are the values, at the equally spaced radial points, of the functions generating the components of $\boldsymbol{H}$. The real V of lowest magnitude is of most interest because, with its associated eigenvector, it represents the most efficient mode of operation of the dynamo. The size of the matrix to be solved is the limiting factor of the process, for if it cannot all be stored in a machine core the time taken to solve it becomes prohibitively long.

Matrix size has been kept to a minimum by examining flow patterns that are selective in the number of magnetic field components they involve. A general flow will involve all components of magnetic field; however, it is fortunate that the interactions of some flow patterns are such that the magnetic harmonics can be divided into distinct groups. There are then interactions within each group, but not between different groups, and just one group can be examined by itself, under the condition that the members of the other groups are all zero. In this way the number of magnetic components involved is greatly reduced.

The use of perturbation methods or the further development of computing machines may well enable a sufficient number of magnetic components to be taken into account to test a general flow for dynamo action. It should then be practicable to investigate the flows that, from examination of the geomagnetic secular variation, have been deduced to exist in the core of the Earth.

4. Results for the Bullard–Gellman flow pattern

When a computing routine as involved as that just described is used, great care must be taken that no errors in logic are present. Once the matrix has been formed, the accuracy of its solution is easily checked by comparing the two products of matrix by eigenvector and eigenvalue by eigenvector. However, during the formation of the matrix no easy check is possible, and great importance has therefore been laid in the re-calculation of previously published results, to make sure that the new ones agree with them.

Table 1 gives the results for the cases tested from Bullard & Gellman (1954). Exactly the same method was followed in forming the matrix, and the small differences in the values for V are taken to indicate different degrees of accuracy in the iterative procedures used to solve it. Table 2 compares results with Gibson & Roberts (1969). These results are from two distinct methods of solving the differential equations, as Gibson & Roberts used Chebychev collocation, rather

TABLE 1. COMPARISON OF SOME RE-CALCULATIONS WITH THE RESULTS OF BULLARD & GELLMAN

Case 1

number of terms taken in the series for the magnetic field = 4
number of parts of division of the radius = 10
flow derived from the radial functions $S_2^{2c}(r) = r^3(1-r)^2$; $T_1(r) = 10r^2(1-r)$
Bullard & Gellman's result: $V = 47.50$
result of re-calculation: $V = 47.59$

Case 2

number of terms taken in the series for the magnetic field = 4
number of parts of division of the radius = 10
flow derived from the radial functions $S_2^{2c}(r) = r^3(1-r)^2$; $T_1(r) = 100r^2(1-r)$
Bullard & Gellman's result: $V = 42.1$
result of re-calculation: $V = 42.10$

Case 3

number of terms taken in the series for the magnetic field = 7
number of parts of division of the radius = 10
flow derived from the radial functions $S_2^{2c}(r) = r^3(1-r)^2$; $T_1(r) = 5r^2(1-r)$
Bullard & Gelman's result: $V = 68.8$
result of re-calculation: $V = 67.6$

TABLE 2. COMPARISON OF RESULTS WITH THOSE OF GIBSON & ROBERTS

The flow pattern is derived from the radial functions

$$S_2^{2c}(r) = r^3(1-r)^2, \quad T_1(r) = 5r^2(1-r);$$

b is the number of terms taken in the series expansion of the magnetic field. n is the degree of the last term in the series for the magnetic field. The values given in brackets after the new results are the number of parts into which the radius was divided for numerical solution of the differential equations.

n	b	Gibson & Roberts's value for V	result for V reported in this paper
2	4	66.5	58.6 (10 parts); 64.4 (20 parts)
3	5	62.9	
3	7	83.1	67.6 (10 parts); 78.5 (20 parts)
4	8	70.3	
4	10	72.7	
4	12	75.9	93.9 (15 parts); 94.3 (17 parts)
5	13	63.0	
5	15	120.4	110.6 (12 parts)
5	17	143.2	

than difference expressions. Both methods should give the same result in the limit, which in the present treatment is the very fine division of radius. In view of the different methods of solution, the eigenvalues for V are in reasonable agreement, with the exception of the case for $n = 4$ and $b = 12$, where 94.3 conflicts with 75.9. No explanation of this discrepancy can be offered, and one of the results must be in error.

Table 3. Further results for a particular Bullard & Gellman flow pattern

The flow is derived from the radial functions

$$S_2^{2c}(r) = r^3(1-r)^2, \qquad T_1(r) = 10r^2(1-r);$$

b is the number of terms taken in the series expansion for $\boldsymbol{H}$. n is the degree at which the series for $\boldsymbol{H}$ is truncated. The values of M are the number of parts into which the radius was divided for numerical solution of the differential equations.

n	b	V for $M = 12$	V for $M = 14$
2	4	49.3	50.4
3	7	67.3	70.2
4	12	72.8	75.0
5	17	95.3	102.3

The greatest significance of table 2 is that the eigenvalues are not converging as more terms are included in the series expansion of the magnetic field. Truncation of the series has not, therefore, been shown to be justified, and dynamo action for this $T_1S_2^{2c}$ flow cannot be claimed. A case with a slightly different ratio between the two components of velocity has also been tested: the results are given in table 3, and again the eigenvalues for V have not stabilized. Analysis of what is happening is helped by inspection of the eigenvectors for each level of truncation, and these are given in figure 1.

It appears that the inclusion of higher harmonics reduces the efficiency of the dynamo action between the lower harmonics, by causing too much energy to be drawn from them. In column (a) T_2 is the dominant harmonic; however, in column (d) T_4 is dominant, generating a maximum field strength an order of magnitude greater than that of T_2.

5. Results for a flow pattern of three components

The evident failure of the $T_1S_2^{2c}$ flow pattern to act as a dynamo is probably related to a theorem proved by Braginskii (1964). He considered a dynamo in which the motion is almost cylindrically symmetrical, in the sense that the unsymmetrical component of velocity is a perturbation superimposed on the symmetrical velocity. In the limit when this perturbation is very small, dynamo action can occur only if the unsymmetrical part of the motion contains spherical harmonics with both sine and cosine dependence upon longitude. $T_1S_2^{2c}$ does not satisfy this criterion, as the only unsymmetrical component is S_2^{2c} of cosine dependence. Tough (1967) has extended Braginskii's work to the next order in the perturbation analysis. Their arguments leave uncertain whether $T_1S_2^{2c}$ will work as a dynamo when the S_2^{2c} velocity component is not merely a perturbation:

Figure 1. Radial functions of the components of magnetic field, obtained by solving the dynamo equation for $T_1S_2^{2c}$ flow at four different levels of truncation. Column (a) is the solution for truncation of harmonics above second degree, (b) above third degree, (c) above fourth degree, and (d) above fifth degree. There is little evidence that the radial functions stabilize as the degree of truncation is increased.

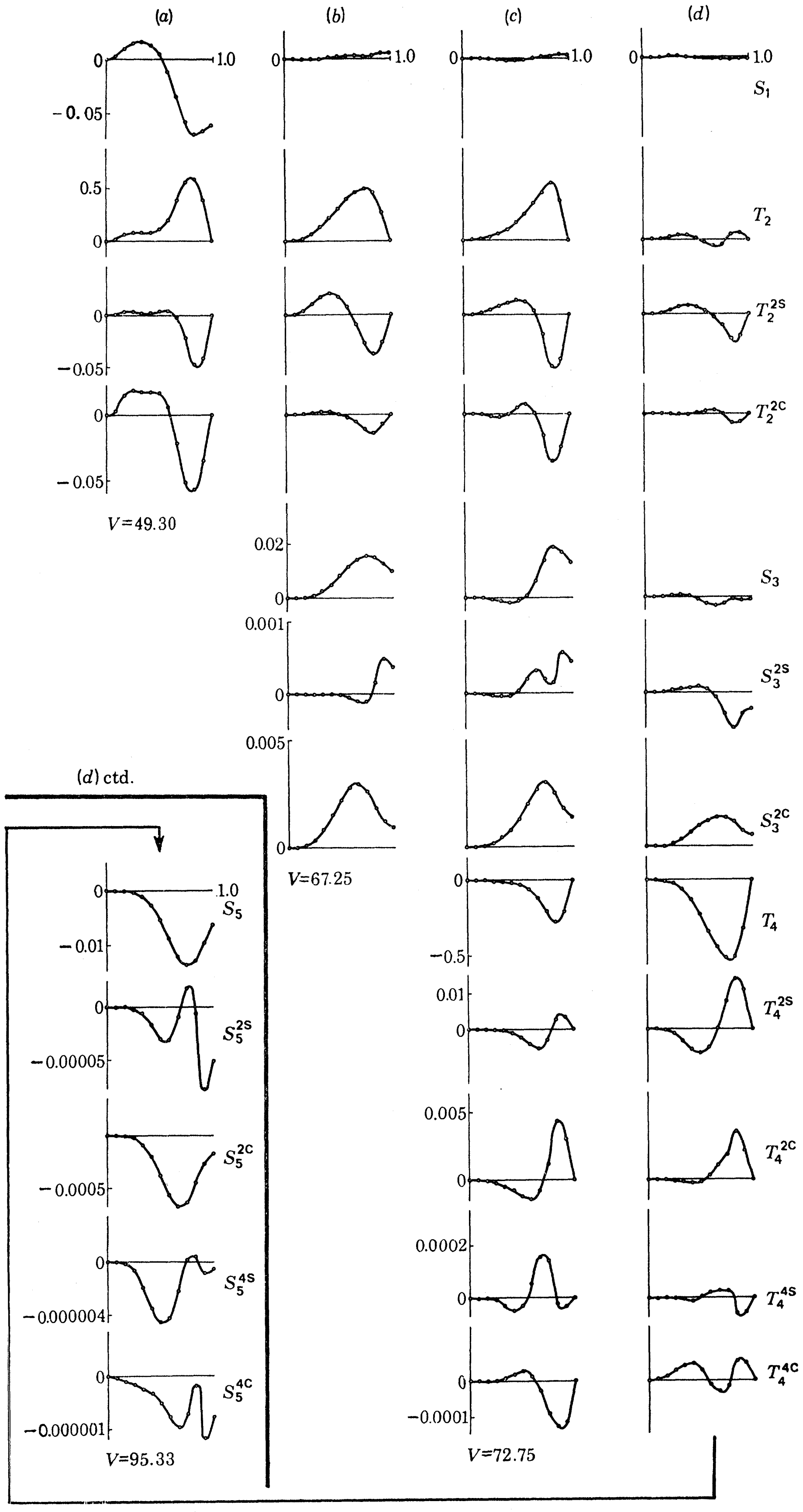

Figure 1. For legend see facing page.

however, the failure of the numerical work to converge supports the suggestion by Tough that their theorem may be stronger than it has yet been proved to be.

If an S_2^{2s} component is added to the $T_1 S_2^{2c}$ pair, the symmetry of the flow pattern is reduced, and Braginskii's condition, requiring both sine and cosine dependence upon longitude, is satisfied. A great number of other flow patterns also satisfy the condition, but $T_1 S_2^{2c} S_2^{2s}$ is especially suitable for a Bullard–Gellman analysis because, like $T_1 S_2^{2c}$, it has a relatively simple interaction diagram. The S_2^{2s} flow adds interactions between magnetic field components that are already in the $T_1 S_2^{2c}$ interaction diagram, but no new magnetic field components become involved. This is important because the order of the matrix to be ultimately solved depends on the number of magnetic components, but not on the number of interactions.

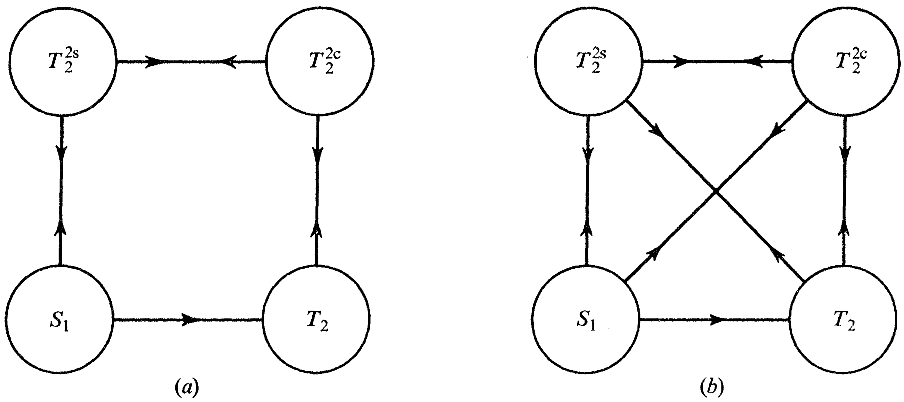

FIGURE 2. The interactions between magnetic field components of first and second degree, caused by the fluid flow. (*a*) is for $T_1 S_2^{2c}$ flow, (*b*) is for $T_1 S_2^{2c} S_2^{2s}$ flow. The horizontal connexions are caused by the T_1 component of flow, the vertical by the S_2^{2c} component, and the diagonal by the S_2^{2s} component. A line connecting two circles means that the flow component represented by the line acts on the magnetic component in the first circle to produce the magnetic component in the second circle. Interactions with higher field harmonics would also connect with the diagrams.

The type of extra interaction introduced by the S_2^{2s} flow is illustrated in figure 2, where the interactions caused by the $T_1 S_2^{2c}$ and $T_1 S_2^{2c} S_2^{2s}$ flows are compared, for magnetic harmonics of first and second degree. A full table of the $T_1 S_2^{2c} S_2^{2s}$ interactions that have been taken into account is given in table 4. The table could be extended indefinitely to include interactions with higher harmonics.

The radial functions for the T_1, S_2^{2c}, and S_2^{2s} flow components have been chosen rather arbitrarily within the limitations of the boundary conditions as given by Bullard & Gellman. The following have been used:

$$\begin{aligned}
T_1(r) &= 10r^2(1-r^2), \\
S_2^{2c}(r) &= r^3(1-r^2)^2, \\
S_2^{2s}(r) &= 1.6r^3(1-4r^2)^2 \quad (0 \leqslant r \leqslant 0.5), \\
S_2^{2s}(r) &= 0 \qquad\qquad\qquad (0.5 < r \leqslant 1),
\end{aligned}$$

TABLE 4. INTERACTION DIAGRAM FOR A $T_1 S_2^{2c} S_2^{2s}$ FLOW PATTERN

1, 2 and 3 denote interactions due to the T_1, S_2^{2c} and S_2^{2s} components of flow respectively. The dark lines show different levels of truncation.

component of magnetic field being acted on

	S_1	T_2	T_2^{2s}	T_2^{2c}	S_3	S_3^{2s}	S_3^{2c}	T_4	T_4^{2s}	T_4^{2c}	T_4^{4s}	T_4^{4c}	S_5	S_5^{2s}	S_5^{2c}	S_5^{4s}	S_5^{4c}	T_6	T_6^{2s}	T_6^{2c}	T_6^{4s}	T_6^{4c}	T_6^{6s}	T_6^{6c}	
	.	.	2	3	.	3	2	.	.	.	.	.	.	.	.	.	.	.	.	.	.	.	.	.	S_1
	1	.	3	2	1	2	3	.	3	2	.	.	.	.	.	.	.	.	.	.	.	.	.	.	T_2
	2	3	.	1	2	1	.	3	.	.	2	3	.	.	.	.	.	.	.	.	.	.	.	.	T_2^{2s}
$n = 2$	3	2	1	.	3	.	1	2	.	.	3	2	.	.	.	.	.	.	.	.	.	.	.	.	T_2^{2c}
	.	.	2	3	.	3	2	.	2	3	.	.	.	3	2	.	.	.	.	.	.	.	.	.	S_3
	3	2	.	.	3	.	1	2	.	.	3	2	3	.	.	2	3	.	.	.	.	.	.	.	S_3^{2s}
$n = 3$	2	3	.	.	2	1	.	3	.	.	2	3	2	.	.	3	2	.	.	.	.	.	.	.	S_3^{2c}
	.	.	3	2	1	2	3	.	3	2	.	.	1	2	3	.	.	.	3	2	.	.	.	.	T_4
	.	3	.	.	2	1	.	3	.	1	2	3	2	1	.	3	2	3	.	.	2	3	.	.	T_4^{2s}
	.	2	.	.	3	.	1	2	1	.	3	2	3	.	1	2	3	2	.	.	3	2	.	.	T_4^{2c}
	.	.	2	3	.	3	2	.	2	3	.	1	.	3	2	1	.	.	2	3	.	.	2	3	T_4^{4s}
$n = 4$	.	.	3	2	.	2	3	.	3	2	1	.	.	2	3	.	1	.	3	2	.	.	3	2	T_4^{4c}
	.	.	.	.	.	3	2	.	2	3	.	.	.	3	2	.	.	.	2	3	.	.	.	.	S_5
	.	.	.	.	3	.	.	2	.	.	3	2	3	.	1	2	3	2	.	.	3	2	.	.	S_5^{2s}
	.	.	.	.	2	.	.	3	.	.	2	3	2	1	.	3	2	3	.	.	2	3	.	.	S_5^{2c}
	.	.	.	.	.	2	3	.	3	2	.	.	.	2	3	.	1	.	3	2	.	.	3	2	S_5^{4s}
$n = 5$	.	.	.	.	.	3	2	.	2	3	.	.	.	3	2	1	.	.	2	3	.	.	2	3	S_5^{4c}
	.	.	.	.	.	.	.	.	3	2	.	.	1	2	3	.	.	.	3	2	.	.	.	.	T_6
	.	.	.	.	.	.	.	3	.	.	2	3	2	1	.	3	2	3	.	1	2	3	.	.	T_6^{2s}
	.	.	.	.	.	.	.	2	.	.	3	2	3	.	1	2	3	2	1	.	3	2	.	.	T_6^{2c}
	.	.	.	.	.	.	.	.	2	3	.	.	.	3	2	1	.	.	2	3	.	1	2	3	T_6^{4s}
	.	.	.	.	.	.	.	.	3	2	.	.	.	2	3	.	1	.	3	2	1	.	3	2	T_6^{4c}
	.	.	.	.	.	.	.	.	.	.	2	3	.	.	.	3	2	.	.	.	2	3	.	1	T_6^{6s}
$n = 6$	.	.	.	.	.	.	.	.	.	.	3	2	.	.	.	2	3	.	.	.	3	2	1	.	T_6^{6c}

component of magnetic field being produced which are shown plotted over the range of unit radius in figure 3. The radial function for S_2^{2s} must be different from the S_2^{2c} function if the two flow patterns are to be physically different, and $S_2^{2s}(r)$ has been limited within the inner half of the radius merely as a simple way of achieving this. The streamlines of the $T_1 S_2^{2c} S_2^{2s}$ combination form a complicated family of curves in a sphere. They can, however, be drawn in the equatorial plane, for there they are two-dimensional, owing to the $\hat{\theta}$-components of velocity being zero. Streamlines in the equatorial plane are shown in figure 4*a*–*e*. The component flow patterns are drawn separately and combined, and for comparison the $T_1 S_2^{2c}$ flow of table 3 is also given. It can be seen that the addition of the S_2^{2s} component considerably changes the character of the

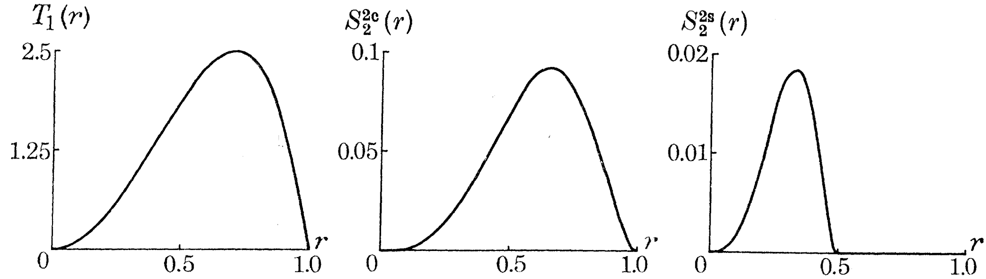

FIGURE 3. The radial functions generating the components of the $T_1 S_2^{2c} S_2^{2s}$ flow. (*a*) $T_1(r)$, (*b*) $S_2^{2c}(r)$, and (*c*) $S_2^{2s}(r)$.

flow pattern. The streamlines of figure 4*d* for the $T_1 S_2^{2c} S_2^{2s}$ flow are divided into two regimes. In the outer regime the S_2^{2s} flow has no effect, and the streamlines are of regular $T_1 S_2^{2c}$ form. The boundary between the outer and inner regimes is formed by the $T_1 S_2^{2c}$ streamline that just touches the $r = 0.5$ circle. In the inner regime, the streamlines leave the critical $T_1 S_2^{2c}$ streamline asymptotically, to spiral in and close, again asymptotically, on one of two stagnation points. In this case the equatorial streamlines are not typical of the flow, and in figure 4*f* a projection onto the equatorial plane is given for a $T_1 S_2^{2c} S_2^{2s}$ streamline in the upper hemisphere. The projection is vertical, and the height of the streamline above the equatorial plane is given at a number of points, to help the viewer form an impression of its three-dimensional whirling nature.

Results for the analysis of the $T_1 S_2^{2c} S_2^{2s}$ flow pattern are given in table 5, as eigenvalues for V. Each value represents the solution of a matrix, and the extent of the table has been limited in two ways by the necessity of keeping matrix size within computing capacity. One limitation has been on the number of parts of division of radius, in the numerical solution of the differential equations. This has prevented taking the lower lines of the table further to the right. The other limitation has been on the number of harmonics able to be taken in the series for $\boldsymbol{H}$. For this reason the table does not extend beyond harmonics of the sixth degree. This is the more critical limitation, as a demonstration of dynamo action depends

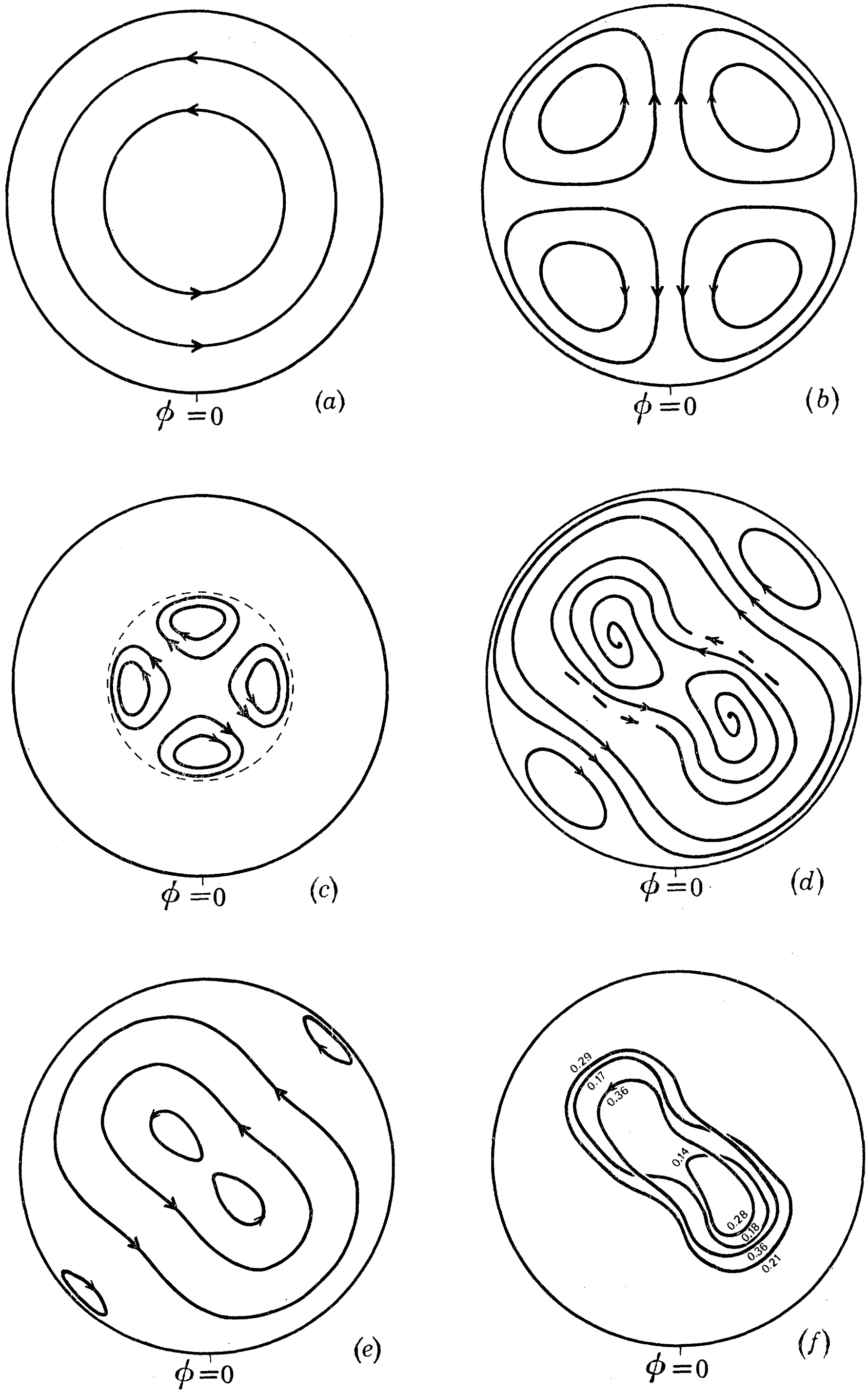

FIGURE 4. (*a*)–(*e*) are streamlines in the equatorial plane of a sphere for the following flows: (*a*) T_1, (*b*) S_2^{2c}, (*c*) S_2^{2s}, (*d*) $T_1 S_2^{2c} S_2^{2s}$, (*e*) $T_1 S_2^{2c}$ as used by Bullard & Gellman. (*f*) is the projection, onto the equatorial plane, of a $T_1 S_2^{2c} S_2^{2s}$ streamline in the upper hemisphere. Its height above the equatorial plane is marked at certain places. The radial functions from which the flows are derived are as given in table 5, except for (*e*) which is given in table 3.

TABLE 5. EIGENVALUE, V, RESULTS FOR A FLOW OF THREE COMPONENTS DERIVED FROM THE RADIAL FUNCTIONS:

$$T_1(r) = 10r^2(1-r^2),$$
$$S_2^{2c}(r) = r^3(1-r^2)^2,$$
$$S_2^{2s}(r) = 1.6r^3(1-4r^2)^2 \quad (0 \leqslant r \leqslant 0.5),$$
$$S_2^{2s}(r) = 0 \quad (0.5 < r \leqslant 1).$$

The number of terms taken in the expansion for $\boldsymbol{H}$ is denoted by b.
The degree of truncation of the series is denoted by n.
The total number of interactions involved is denoted by I.
The number of parts into which the radius is divided is denoted by M.

n	b	I	V								
			$M = 10$	$M = 12$	$M = 14$	$M = 16$	$M = 18$	$M = 20$	$M = 22$	$M = 24$	$M = 26$
2	4	11	22.66	23.75	24.45	24.92	25.25	25.50	25.70	25.85	25.97
3	7	32	12.24	15.31	18.63	22.28	26.30	30.58	34.58	37.75	39.91
4	12	83	11.50	13.72	15.82	17.76	.	.	.	.	.
5	17	144	12.69	15.56	18.41	21.28	.	.	.	.	.
6	24	239	.	.	.	20.73	.	.	.	.	.

on enough terms being taken in the series for $\boldsymbol{H}$ for a stable solution to be obtained. However, in table 5, it does appear that a stable solution has been reached. For $M = 16$, in the step in truncation from fifth to sixth degree, the eigenvalue changes from 21.28 to only 20.73 even though the number of harmonics increases from seventeen to twenty-four, and the number of interactions involved is almost doubled. This is to be contrasted with the steady increase in tables 2 and 3 for the $T_1 S_2^{2c}$ flow.

If the addition of higher degree harmonics is having little effect on the eigenvalues, the eigenvectors also should be little changed. Four sets of eigenvectors are given in figure 5, corresponding to four of the eigenvalues of table 5 in the $M = 12$ column. Again computing facilities have prevented eigenvectors being found for the $M = 16$ column, and for $n = 6$. Nevertheless, figure 5 shows quite clearly that the important lower harmonics appear to be stable by the time truncation has reached the fifth degree. Indeed, inspection of figure 5 gives considerable insight into how the dynamo works. As in figure 1 for the $T_1 S_2^{2c}$ flow, the S_1 function is greatly changed by inclusion of the higher harmonics, being weakened by an order of magnitude and even changing sign. The strength of the dynamo appears to lie in the T_2, T_2^{2s}, and T_2^{2c} harmonics, which have stabilized in figure 5, though not in figure 1. The kernel of dynamo action therefore appears to be the T_2–T_2^{2s}–T_2^{2c}–T_2 triangle of interactions, which can be seen as part of figure 2b.

FIGURE 5. Radial functions of the components of magnetic field, obtained as eigenvectors for the $T_1 S_2^{2c} S_2^{2s}$ flow. Column (a) is the solution for truncation above second degree, (b) above third degree, (c) above fourth degree, and (d) above fifth degree.

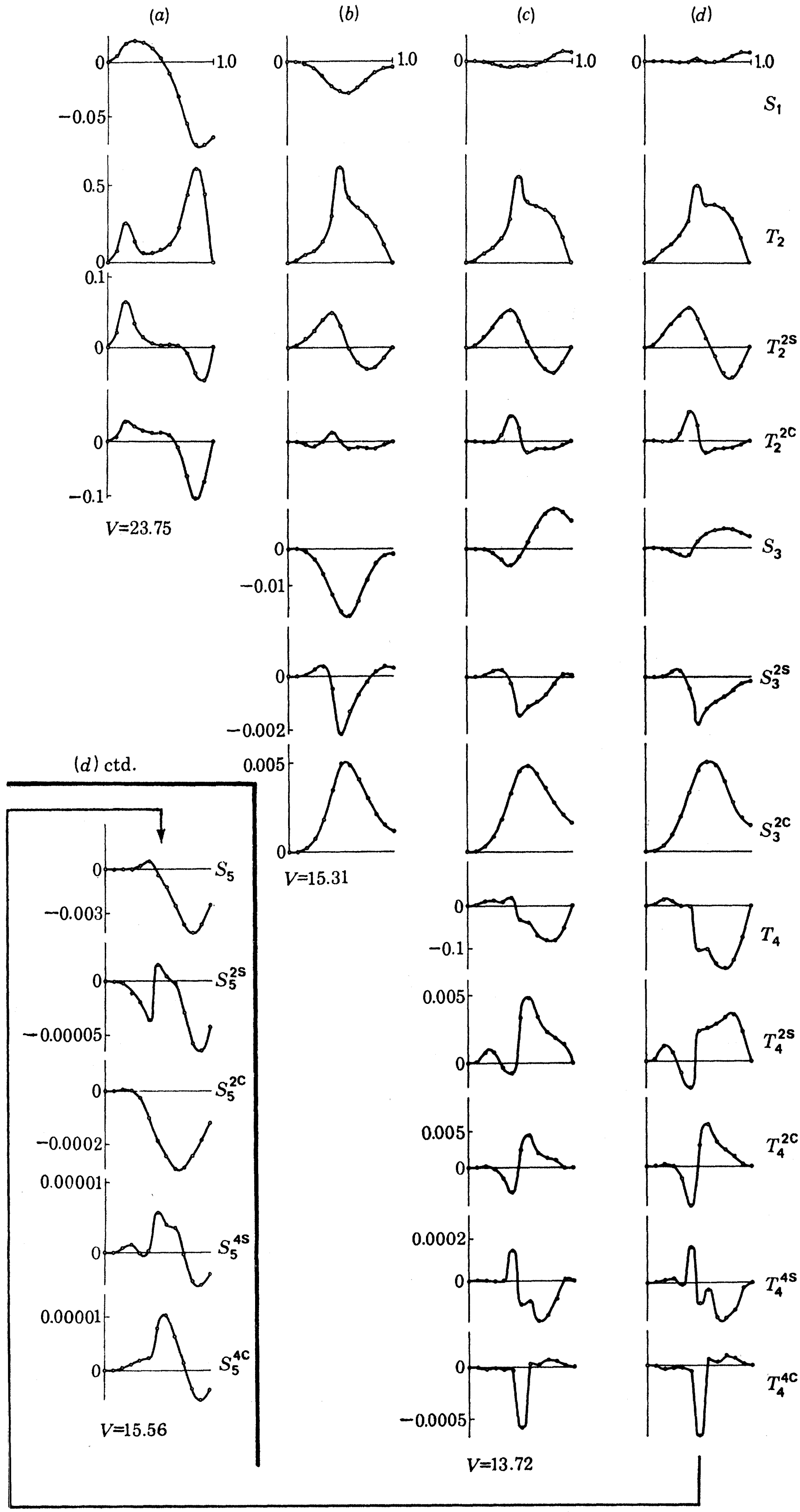

Figure 5. For legend see facing page.

6. Conclusions

A Bullard–Gellman analysis, carried out on a $T_1 S_2^{2c} S_2^{2s}$ flow pattern, has produced results which are strong evidence that this motion will maintain dynamo action. No such conclusion can be drawn for the more symmetrical $T_1 S_2^{2c}$ flow pattern, and Braginskii's rule, that a dynamo must exhibit both sine and cosine dependence on longitude, is substantiated.

The $T_1 S_2^{2c} S_2^{2s}$ flow was chosen for analysis because it has a relatively simple interaction diagram. The flow in the fluid core of the earth is not known; that it acts as a dynamo is, however, the most probable cause of the Earth's magnetic field. The dynamo process may be similar to that of the $T_1 S_2^{2s} S_2^{2c}$ flow, and the results of this paper therefore have implications for geomagnetism. One aspect of the results is of particular interest.

Examination of figure 5 shows that the main magnetic components of the $T_1 S_2^{2c} S_2^{2s}$ dynamo are toroidal and, indeed, it has been separately found that the T_2–T_2^{2s}–T_2^{2c}–T_2 loop of figure 2*b* can act as a dynamo by itself when all other interactions are ignored. The possibility is thus established that the dominant components of the geomagnetic dynamo are similarly toroidal, and lie completely within the core. The dipole and 'non-dipole' fields, observed on the surface of the Earth and arising from the S_1 and other poloidal harmonics, then become of subsidiary importance in the dynamo process, and may change with time, even reverse, just as perturbation effects of the main interactions between the toroidal components. Such changes would of course be time dependent phenomena, however the manner of change might be analogous to the variation from column *b* to column *c* in figure 5, where S_1 has reversed without any associated change in the character of T_2, T_2^{2s}, and T_2^{2c}.

The author would first like to express his gratitude to Professor Sir Edward Bullard, F.R.S., of Cambridge, who suggested to him that the work be undertaken, who has been a constant source of encouragement and guidance, and who kindly reviewed the first draft of this paper. It is a pleasure, also, to acknowledge the interest and help of Professor P. H. Roberts of Newcastle upon Tyne. Mr S. Scott has greatly assisted by providing his computing routines for Gaunt and Elsasser integrals. Programs for finding the eigenvalues and eigenvectors of general non-symmetric matrices came from the Harwell Program Library. Dr R. Hide once suggested to the author the idea that the dipole field of the earth may reverse without the toroidal components changing sign.

This project has involved a great deal of computing, carried out on three continents. The author is grateful to Dr R. S. Anderssen, Dr J. C. Cain and Dr S. J. Cain, Miss J. M. Rohl, Mr N. J. Butler, Mr B. F. Butterfield, Mr P. N. Creasy, Mr I. R. Simpson, Mr R. Thirlby and Mr P. Tindale for assistance. Eigenvalues of the largest matrix solved, of order three hundred and sixty, were determined using an IBM 360/91 machine at the Goddard Space Flight Center, Maryland.

A major portion of the work was done while the author held a Canadian National Research Council post-doctoral fellowship at the Department of Geodesy and Geophysics at Madingley Rise, Cambridge. For this he is most grateful, and he would also like to acknowledge that his initial interest in the magnetic field in the core was stimulated while he was working with Professor C. M. Carmichael at the University of Western Ontario.

REFERENCES

Backus, G. 1958 *Ann. Phys.* **4**, 372.

Braginskii, S. I. 1964 *J. Exp. Theor. Phys.* (*U.S.S.R.*) **47**, 1084. Trans.: *Soviet Phys. J.E.T.P.* **20**, 726 (1965).

Bullard, E. C. & Gellman, H. 1954 *Phil. Trans. Roy. Soc. Lond.* A **247**, 213.

Cowling, T. G. 1933 *Mon. Not. R. astr. Soc.* **94**, 39.

Elsasser, W. M. 1946 *Phys. Rev.* **69**, 106.

Gibson, R. D. & Roberts, P. H. 1969 In *The application of modern physics to the Earth and planetary interiors*, pp. 577–602 (ed. S. K. Runcorn). London: Wiley.

Herzenberg, A. 1958 *Phil. Trans. Roy. Soc. Lond.* A **250**, 543.

Lortz, D. 1968 *Phys. Fluids* **11**, 913.

Lowes, F. J. & Wilkinson, I. 1963 *Nature, Lond.* **198**, 1158.

Lowes, F. J. & Wilkinson, I. 1968 *Nature, Lond.* **219**, 717.

Tough, J. G. 1967 *Geophys. J. R. astr. Soc.* **13**, 393.